Electronic Supplementary Material (ESI) for ChemComm.

Supporting Information

A Napthalimide Derived Fluorescence Sensor for Solid-Phase Screening of Cucurbit[7]uril-Guest Interactions

Gyan Hari Aryal[a‡], Cooper Hawkins Battle[a‡], Tod A. Grusenmeyer[a], Mengyuan Zhu[a], Janarathanan Jayawickramarajah[a*]

[a] Department of Chemistry Tulane University, 2015 Percival Stern Hall, New Orleans, Louisiana

Table of Contents

1. Experimental Section

1.1. General methods

Unless otherwise stated, all chemicals and solvents were purchased from Sigma Aldrich, TCI America, and Fisher Scientific and used without further purification. Biotin-PEG3-Azide conjugate was obtained from Sigma Aldrich. Cucurbit[7]uril CB[7] was purchased from Acros Organics. The concentration of CB[7] was determined by UV-vis titration with cobaltocenium hexapflorophosphate according to literature procedures.[1] NMR spectra were recorded on either a Varian 400 MHz spectrometer or 300 MHz Bruker spectrometer in $CDCl_3$, $DMSOD_6$ or in D_2O. Chemical shifts are reported in parts per million (ppm) and referenced to the residual solvent peaks. Coupling constants (J) are reported in Hertz (Hz). MALDI-TOF spectra were recorded on a Bruker Autoflex3 Matrix Assisted Laser Desorption Ionization-Time of Flight Mass Spectrometer (MALDI-TOF MS). High-resolution mass spectra were recorded at the Department of Chemistry, Indiana University.

Fluorescence spectra were obtained on a Varian Cary Eclipse Fluorescence Spectrophometer with 3000 μL glass cuvettes. General UV-vis spectra were recorded on a Varian Cary 50 Bio UV-Visible spectrophotometer using 1000 μL quartz cuvettes (unless otherwise specified). Guest compounds used for fluorescence displacement titrations both in solution and on the streptavidin surface were obtained from Sigma Aldrich (unless otherwise specified). Compounds N,N-dimethylmorpholine, N,N-dimethylpiperidine and 4-(Adamantan-1-yl-carboxamido)-benzenesulfonamide (AdBenzSulfonamide) were synthesized according to literature procedures.[2, 3]

1.2 Synthesis Overview

1.2.1. Synthesis of NMI 1

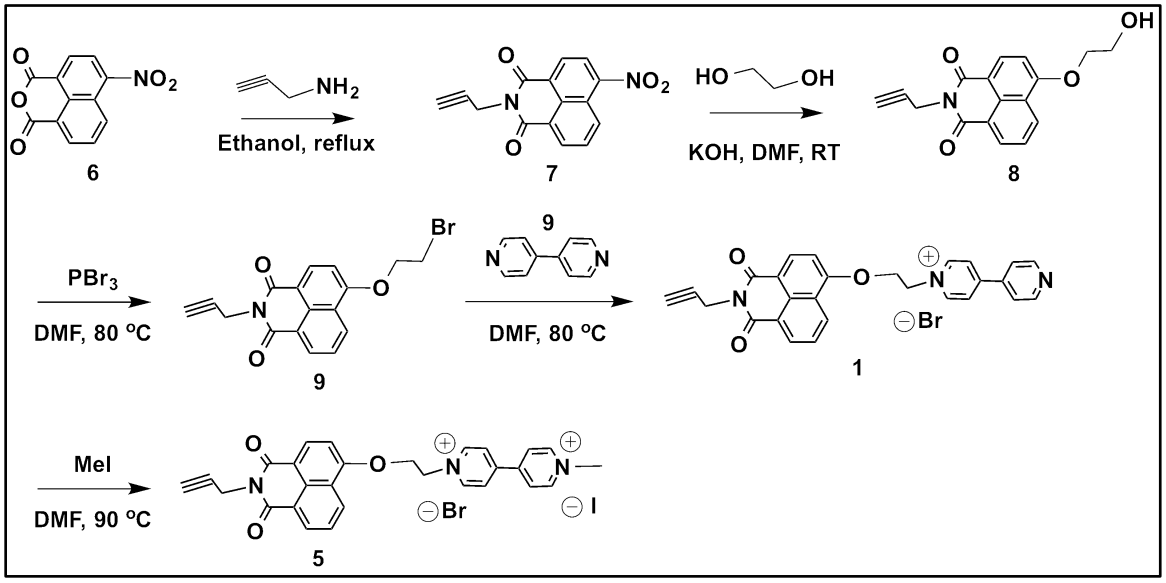

Scheme S1: Synthesis of NMI **1** & NMI **5**

1.2.2. Synthesis of NMI 2

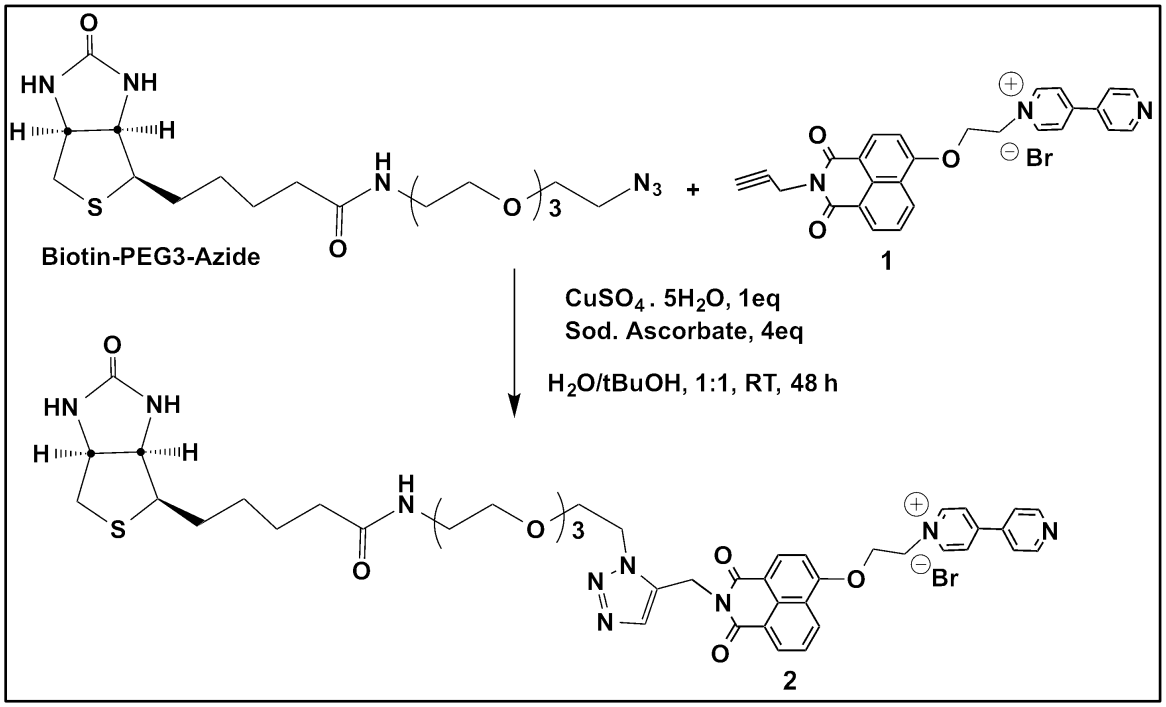

Scheme S2: Synthesis of NMI **2**

1.2.3 Synthesis of 3

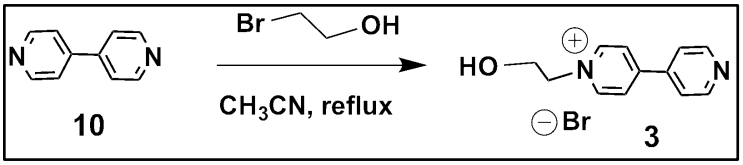

Scheme S3: Synthesis of **3**

1.2.4 Synthesis of NMI 4

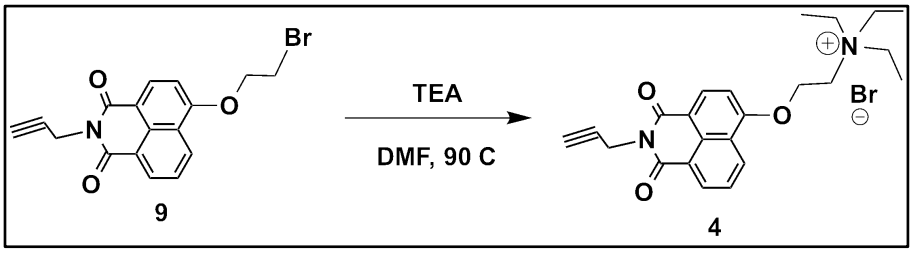

Scheme S4: Synthesis of NMI **4**

1.3. Synthetic Procedures and Characterization

Synthesis of 6-nitro-2-(prop-2-yn-1-yl)-1*H*-benzo[*de*]isoquinoline-1,3(2*H*)-dione (6)

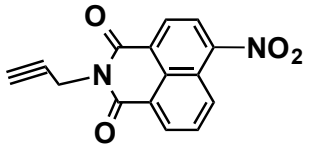

A mixture of 4-Nitro-1,8-napthalic anhydride **5** (500 mg, 2.05 mmol) and propargyl amine (113 mg, 2.07 mmol) in 20 mL of ethanol was refluxed under argon for 3 h at 80 °C. The hot reaction mixture was allowed to cool and precipitate out overnight. The resulting yellow needles were collected using a medium porosity fritted glass filter and washed with ethanol. The solid mass was dried under vacuum (432 mg, 75%). ^{1}H NMR (Varian 400 MHz, $CDCl_3$, 25 ºC): δ 8.85-8.72 (m, 3H), 8.40 (d, *J* = 7.9 Hz, 1H), 7.99 (t, *J* = 8.1 Hz, 1H), 4.95 (s, 2H), 2.21 (s, 1H); ^{13}C NMR (100 MHz, DMSO-d_6) δ 162.1, 161.4, 149.3, 132.0, 130.1, 130.0, 129.1, 128.2, 126.1, 124.3, 122.7, 122.2, 78.8, 73.5, 29.4; HRMS (ESI^+): m/z = 281.0551 $[M+H]^+$ (calc'd. 281.0557 for $C_{15}H_9N_2O_4$).

Synthesis of 6-(2-hydroxyethoxy)-2-(prop-2-yn-1-yl)-1*H*-benzo[*de*]isoquinoline-1,3(2*H*)-dione (7)

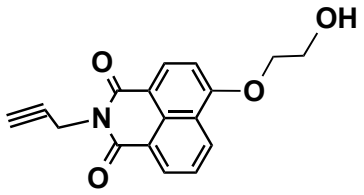

To a stirred solution of **6** (300 mg, 1.07 mmol) in DMF (2mL) was added a pre-mixed solution of KOH (90 mg, 1.6 mmol, 1.5 equiv.) in ethylene glycol (2 mL). The resulting mixture was stirred overnight under argon at room temperature. The reaction mixture was precipitated out with water. The solid mass was collected using a medium porosity fritted glass filter and dried under vacuum (195 mg, 0.66 mmol, 62%). ^{1}H NMR (Varian 400 MHz, $CDCl_3$, 25 ºC): δ 8.65-8.57 (m, 3H), 7.72 (t, *J* = 7.9 Hz, 1H), 7.06 (d, *J* = 8.3 Hz, 1H), 4.94 (s, 2H), 4.40 (t, *J* = 4.2 Hz, 2H), 4.17 (br s, 2H), 2.17 (s, 1H); ^{13}C NMR (100 MHz, DMSO-d_6) δ 162.8, 162.0, 160.1, 133.6, 131.3, 129.1, 128.4, 126.2, 122.8, 121.3, 113.5, 106.9, 79.5, 72.9, 71.0, 59.4, 28.9. HRMS (ESI^+): m/z = 296.0910 $[M+H]^+$ (calc'd. 296.0917 for $C_{17}H_{14}NO_4$).

Synthesis of 6-(2-bromoethoxy)-2-(prop-2-yn-1-yl)-1*H*-benzo[*de*]isoquinoline-1,3(2*H*)-dione (8)

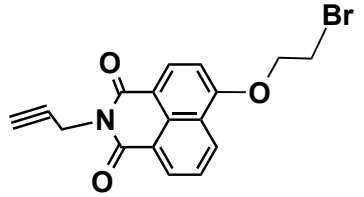

To a solution of **7** (150 mg, 0.50 mmol) in anhydrous DMF (5 mL), PBr_3 (72 μL, 0.76 mmol) was added drop wise. The mixture was stirred under argon at 80 °C overnight. After cooling to room temperature, the mixture was cooled in an ice bath, and then precipitated out with ice-cold water. The solid mass was filtered using medium porosity fritted glass filter, washed with water and dried under vacuum (147 mg, 0.41 mmol, 82%). ^{1}H NMR (Varian 400 MHz, $CDCl_3$, 25 ºC): δ 8.66-8.56 (m, 3H), 7.74 (t, *J* = 7.8 Hz, 1H), 7.01 (d, *J* = 8.2 Hz, 1H), 4.94 (s, 2H), 4.59 (t, *J* = 5.7 Hz, 2H), 3.82 (t, *J* = 5.8 Hz, 2H), 2.17 (s, 1H); ^{13}C NMR (100 MHz, DMSO-d_6) δ 162.7, 162.0, 159.0, 133.4, 131.4, 128.6, 128.4, 126.6, 122.7, 121.4, 114.1, 107.2, 79.5, 72.9, 68.8, 31.1, 28.9. HRMS (ESI^+): m/z = 358.0071 $[M+H]^+$ (calc'd. 358.0073 for $C_{17}H_{13}BrNO_3$).

Synthesis of NMI 1

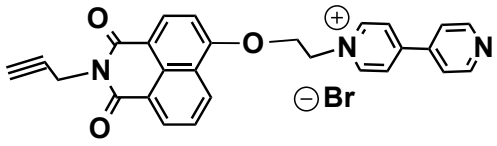

A mixture of **8** (100 mg, 0.28 mmol) and 4,4'-bipyridine (**9**, 250 mg, 1.6 mmol) in anhydrous DMF was stirred at 80 °C under argon overnight. The solvent was removed using a rotary evaporator and the resulting mixture was suspended in ethyl acetate and stirred for two hours. The solid product was collected using a medium porosity fritted glass filter and dried under vacuum (80 mg, 0.16 mmol, 57%). ^{1}H NMR (Varian 400 MHz, DMSO-d_6, 25 ºC): δ 9.49 (d, *J* = 5.8 Hz, 2H), 8.86 (d, *J* = 4.4 Hz, 2H), 8.73 (d, *J* = 5.9 Hz, 2H), 8.64 (d, *J* = 8.2 Hz, 1H), 8.55-8.50 (m, 2H), 8.04 (d, *J* = 4.5 Hz, 2H), 7.87 (t, *J* = 7.7 Hz, 1H), 7.36 (d, *J* = 8.2 Hz, 1H), 5.30 (br s, 2H), 4.93 (br s, 2H), 4.75 (s, 2H), 3.14 (s, 1H). ^{13}C NMR (100 MHz, DMSO-d_6) δ 162.7, 162.0, 158.7, 152.9, 151.0, 150.6, 146.2, 140.8, 133.4, 131.5, 128.9, 126.7, 125.4, 122.6, 122.0, 121.4, 121.3, 114.4, 107.4, 79.4, 73.0, 67.5, 59.4, 29.0. HRMS (ESI$^+$): m/z = 434.1516 $[M]^+$ (calc'd. 434.1505 for $C_{27}H_{20}N_3O_3$).

Synthesis of NMI 2

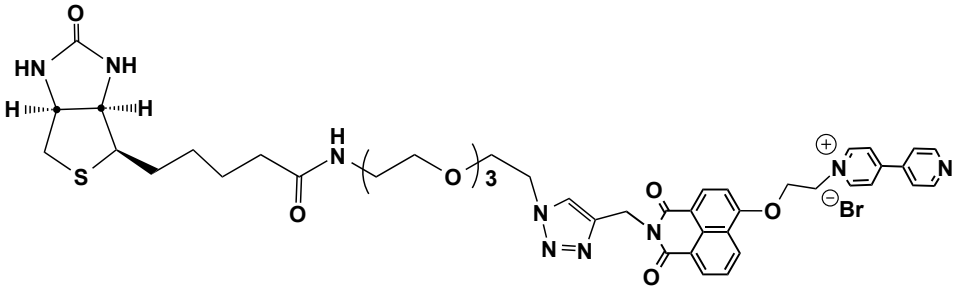

A mixture of **1** (10 mg, 0.02 mmol) and Biotin-PEG_3-Azide (10 mg, 0.02 mmol) was dissolved in a 1:1 mixture of water and *tert*-butyl alcohol (v:v, 14 mL). The mixture was degassed with argon, and then a freshly prepared aqueous solution (0.2 mL) of sodium ascorbate (4.00 equiv.) was added, followed by a solution (0.2 mL) of copper (II) sulphate pentahydrate (1 equiv.). The resulting mixture was stirred under argon at 50 °C for 48 hr and the solvents were removed by rotatory evaporation. The crude sample was analyzed with ^{1}H NMR in DMSO-d_6. Integration of product triazole peak (7.9 ppm) indicates quantitative formation of click product. For more detailed

characterization of the compound, a small portion of the crude sample was further purified via precipitation in 1:1 water/ethanol at 4 ^{o}C overnight. The recovered solid was filtered and dried under vacuum. ^{1}H NMR (Varian 400 MHz, DMSO-d_6, 25 ºC): δ 9.44 (d, *J* = 6.0 Hz, 2H), 8.83 (br s, 2H), 8.69 (d, *J* = 6.0 Hz, 2H), 8.64 (d, *J* = 8.0 Hz, 1H), 8.51-8.45 (m, 2H), 8.01 (br s, 2H), 7.94 (s, 1H), 7.85-7.78 (m, 2H), 7.33 (d, *J* = 8.4 Hz, 1H), 6.38 (s, 1H), 6.33 (s, 1H), 5.23 (br s, 4H), 4.89 (br s, 2H), 4.41 (t, *J* = 4.8 Hz, 2H), 4.25 (m, 1H), 4.03 (m, 1H), 3.72 (t, *J* = 4.8 Hz, 2H), 3.43 (t, *J* = 2.8 Hz, 2H), 3.37-3.31 (m, 8H), 3.10-3.09 (m, 2H), 3.03 (br, 2H), 2.75-2.74 (m, 1H), 2.53 (br, 1H), 2.34 (br, 1H), 2.03 (t, *J* = 7.2 Hz, 2H), 1.60-1.21 (m, 6H). HRMS (ESI^{+}): m/z = 878.3630 $[M]^{+}$ (calc'd. 878.3630 for $C_{45}H_{52}N_9O_8S$).

Synthesis of 1-(2-hydroxyethyl)-[4,4'-bipyridin]-1-ium bromide (3)

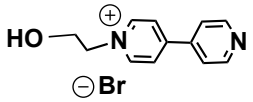

A mixture of 2-bromoethanol (200 mg, 1.6 mmol) and 4,4'-bipyridine (**9**, 250 mg, 1.6 mmol) in acetonitrile (10 mL) was stirred at 80 °C overnight. The resulting precipitate was filtered using medium porosity fritted glass filter and dried under vacuum (202 mg, 0.72 mmol, 45%). ^{1}H NMR (Varian 400 MHz, DMSO-d_6, 25 ºC): δ 9.16 (d, *J* = 6.8 Hz, 2H), 8.86-8.87 (m, 2H), 8.65 (d, *J* = 7.2 Hz, 2H), 8.05-8.04 (m, 2H), 5.29 (br s, 1H), 4.70 (t, *J* = 4.8 Hz, 2H), 3.90 (br s, 2H). ^{13}C NMR (100 MHz, DMSO-d_6) δ 152.3, 151.0, 145.8, 141.0, 125.0, 122.0, 62.6, 60.1. HRMS (ESI^{+}): m/z = 201.1019 $[M]^{+}$ (calc'd. 201.1028 for $C_{12}H_{13}N_2O$).

Synthesis of NMI 4

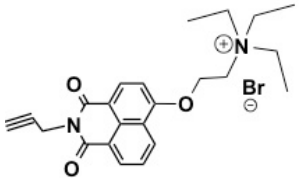

To a solution of compound **8** (200 mg, 0.54 mmol) in DMF (5 mL), triethylamine (500 mg, 4.91 mmol) was added and the mixture was heated at 90 °C for 48 hrs. The mixture was dried using a rotatory evaporator. The solid mass was suspended in ethyl acetate then collected using a medium porosity fritted glass filter. The resulting product was dissolved in water and filtered using fine porosity fritted glass filter. The filtrate was collected and

dried under vacuum (102 mg, 0.22 mmol, 41%). ^{1}H NMR (Varian 400 MHz, D_2O, 25 ºC): δ 8.05 (d, J = 6.8, Hz, 1H), 7.94-7.87 (m, 2H), 7.46 (t, J = 8.0 Hz, 1H), 6.77 (d, J = 8.8 Hz, 1H), 4.66 (s, 2H), 4.55 (br s, 2H), 3.95 (br s, 2H), 3.55 (m, 6H), 2.85 (s, 1H), 1.44 (t, J = 6.8 Hz, 9H). ^{13}C NMR (100 MHz, DMSO-d_6): δ 162.7, 162.0, 159.8, 133.5, 131.12, 128.5, 128.3, 126.2, 122.7, 121.3, 113.4, 106.8, 79.5, 72.9, 68.0, 50.9, 47.1, 28.9, 12.1. HRMS (ESI^{-}): m/z = 379.2033 $[M]^+$ (calc'd. 379.2022 for $C_{23}H_{27}N_2O_3$).

Synthesis of NMI 5

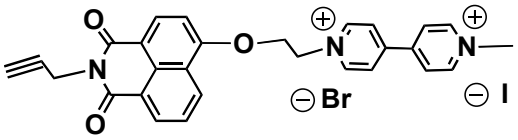

To a stirred solution of **1** (100 mg, 0.19 mmol) in 5 mL DMF, Methyl Iodide (187 mg, 1.31 mmol) was added. The resulting mixture was stirred at 90 °C overnight. After cooling, the reaction mixture was precipitated with ethyl acetate. The solid mass was collected using medium porosity fritted glass filter then dried under vacuum (108 mg, 0.16 mmol, 84%). ^{1}H NMR (Varian 400 MHz, DMSO-d_6, 25 ºC): δ 9.64 (br s, 2H), 9.27 (br s, J = 4 Hz, 2H), 8.87 (br s, 2H), 8.75 (br s, 2H), 8.68 (d, J = 8.8 Hz, 1H) 8.56-8.51 (m, 2H), 7.88 (t, J = 9.6 Hz, 1H), 7.38 (d, J = 7.6 Hz, 1H), 5.35 (br s, 2H), 4.96 (br s, 2H), 4.76 (s, 2H), 4.43 (s, 3H), 3.14 (s, 1H) ppm. HRMS (ESI^{+}): m/z = 449.1735 $[M]^+$ (calc'd. 449.1740 for $C_{28}H_{23}N_3O_3$).

1.3.1: NMR Spectra of Key Compounds

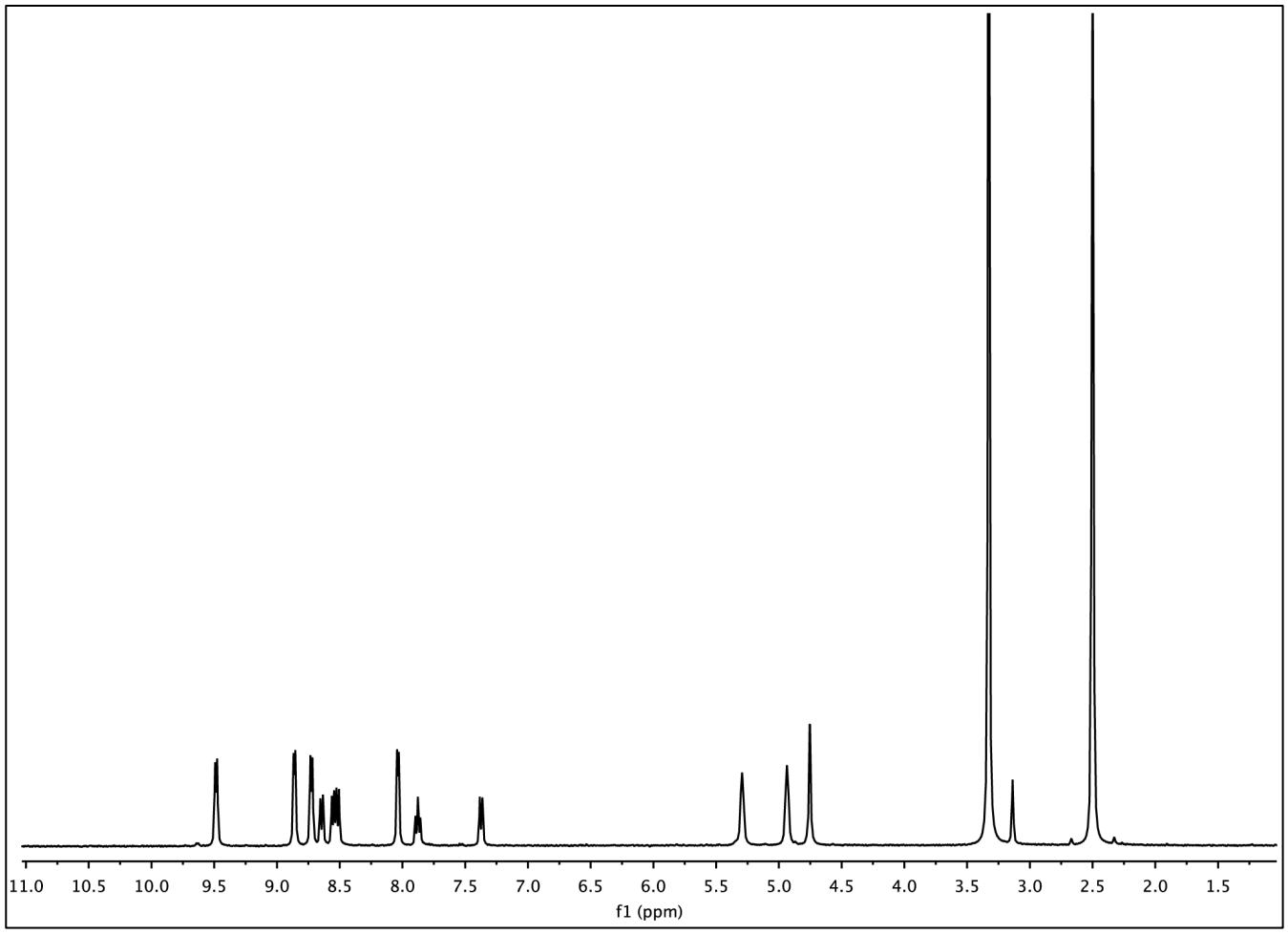

Figure S1: ^{1}HNMR of NMI 1 in DMSO-d_6.

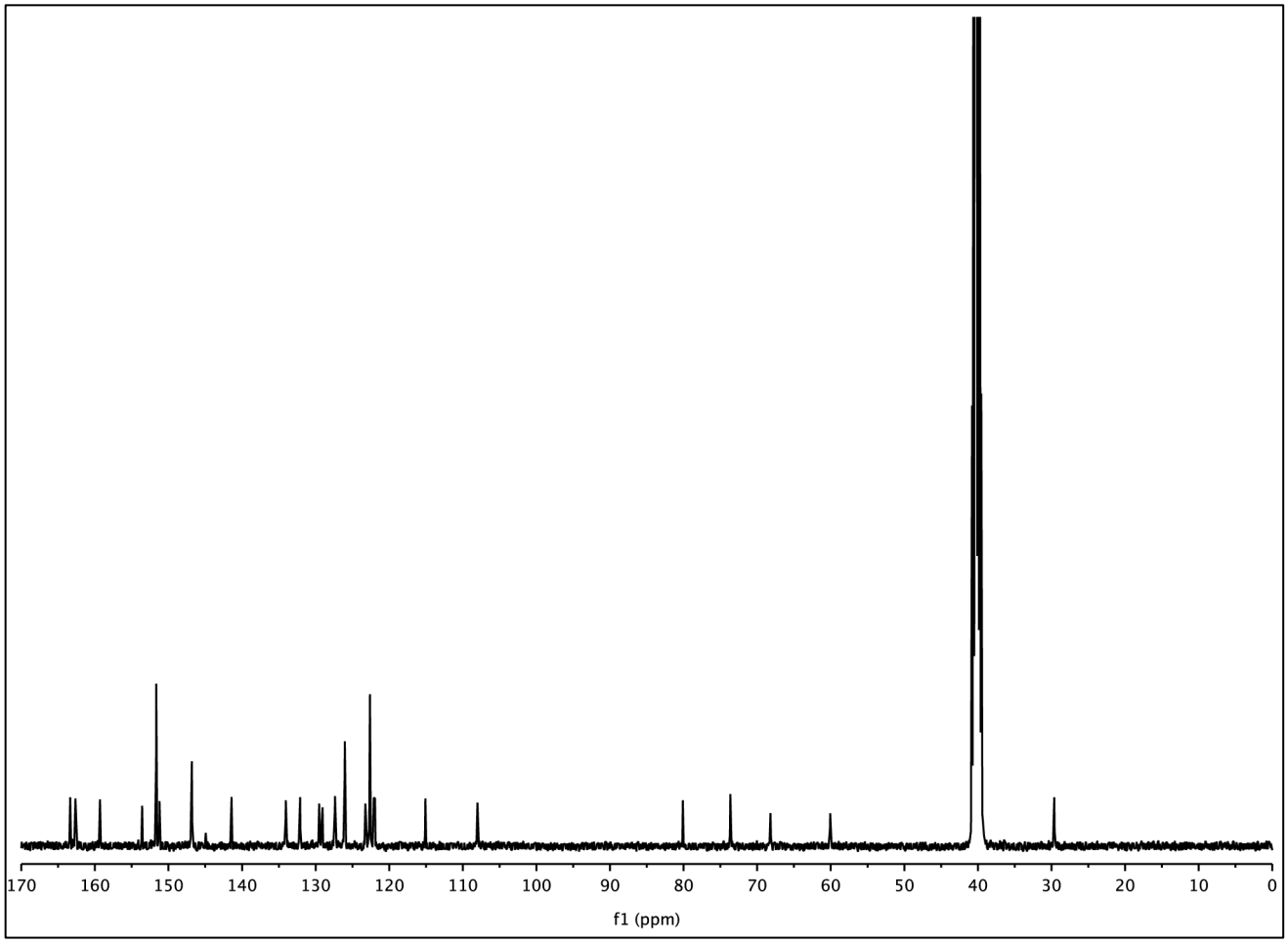

Figure S2: ^{13}CNMR of NMI 1 in DMSO-d_6.

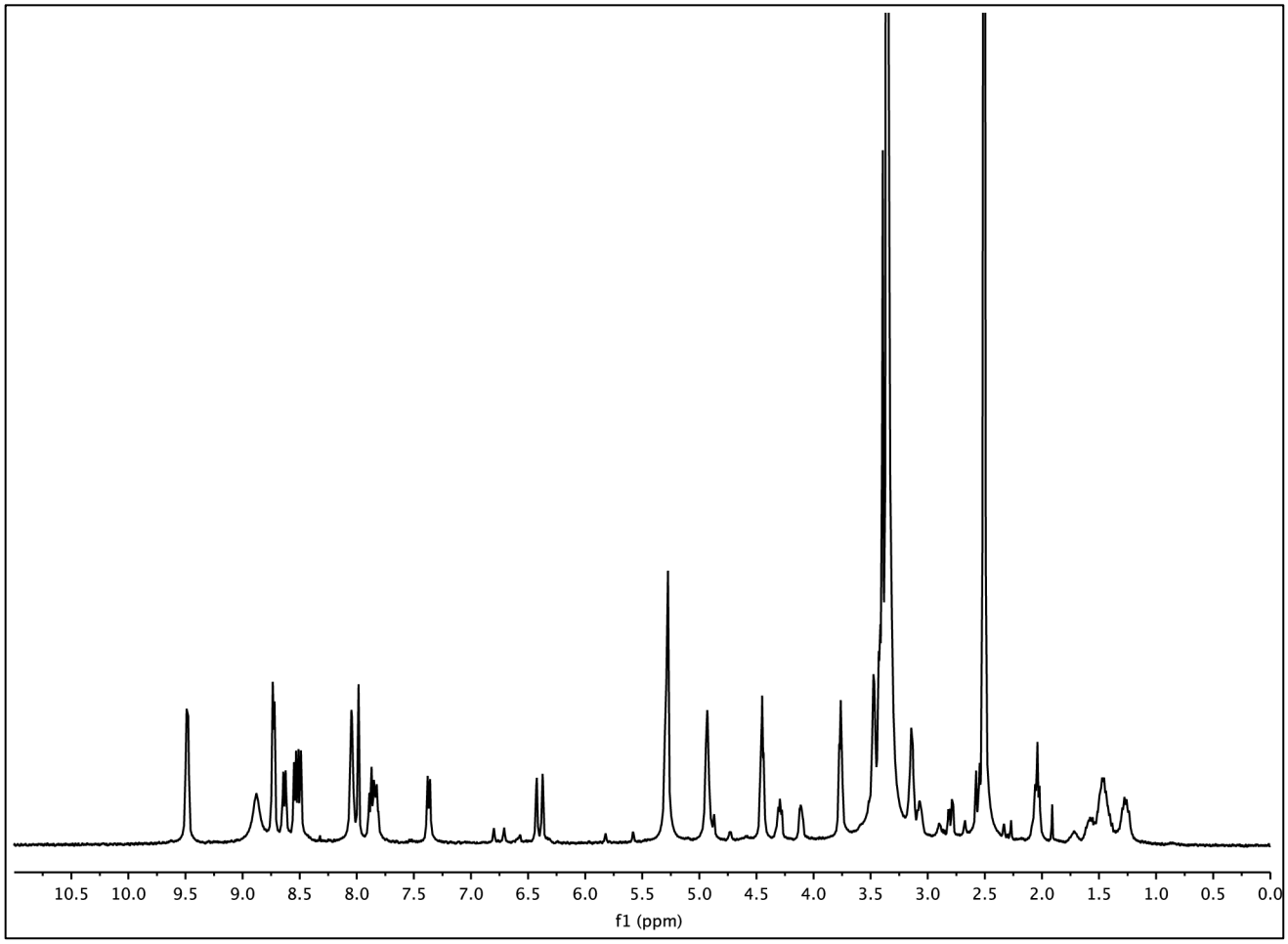

Figure S3: ^{1}HNMR of NMI 2 in DMSO-d_6.

1.4. Mass spectra (MALDI-TOF)

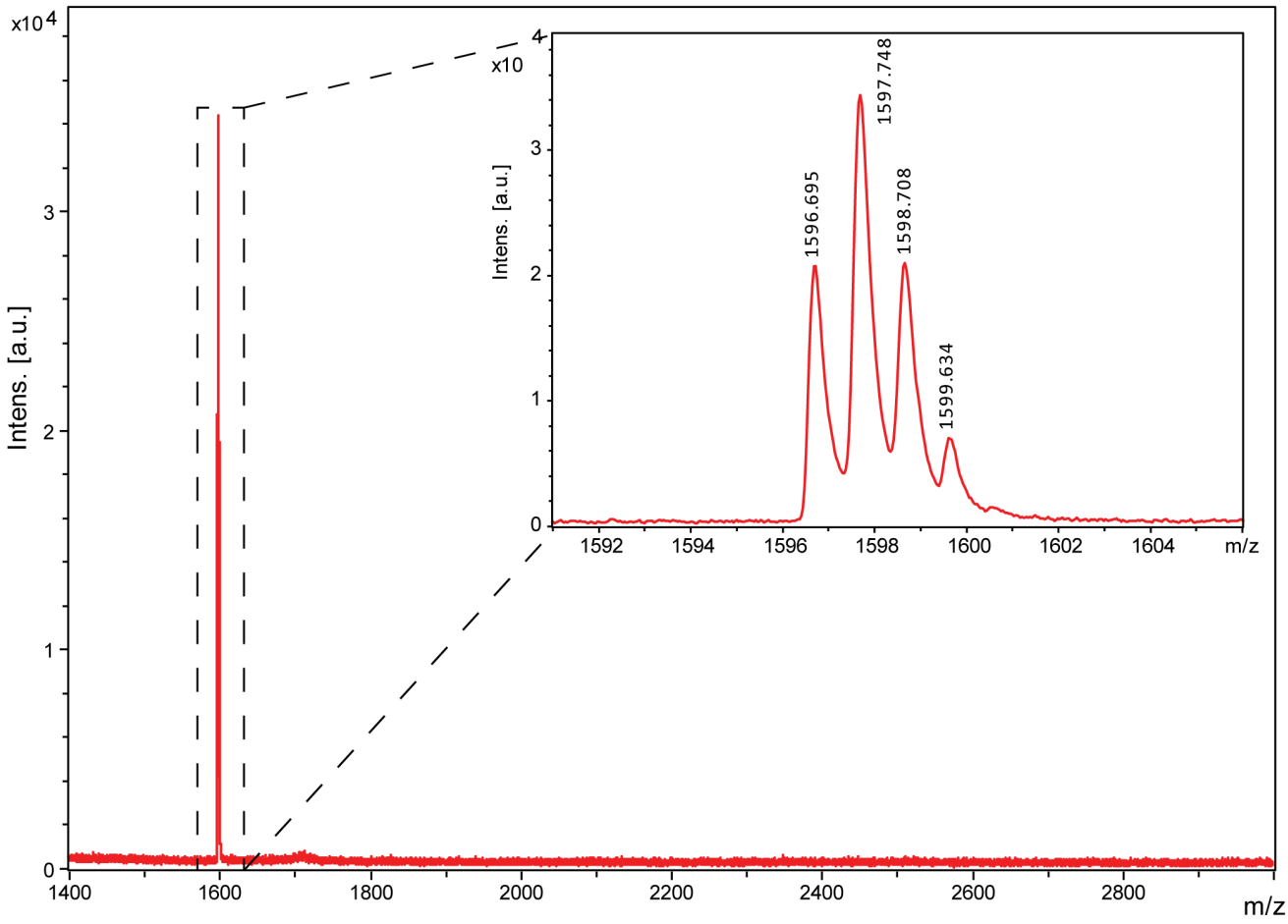

Figure S4. The MALDI-TOF mass spectrum of **1** in the presence of 5-fold excess of CB[7]. Specifically, NMI **1** was mixed with 5 equivalents of CB[7], and spotted onto the target plate. After the sample dried, a 2,5-dihydroxybenzoic acid matrix was applied in a thin layer as a powder. Spectrum collected in in reflector positive mode. $[M]^+$: m/z = 1596.695 (calculated: 1596.493).

Note: The mass at 1596 Da represents a 1:1 complex. With a range up to 3kDa, no higher order complexes are seen.

1.5. UV-vis and Fluorescence spectra

1.5.1. UV-vis study of 1, 3, and 4

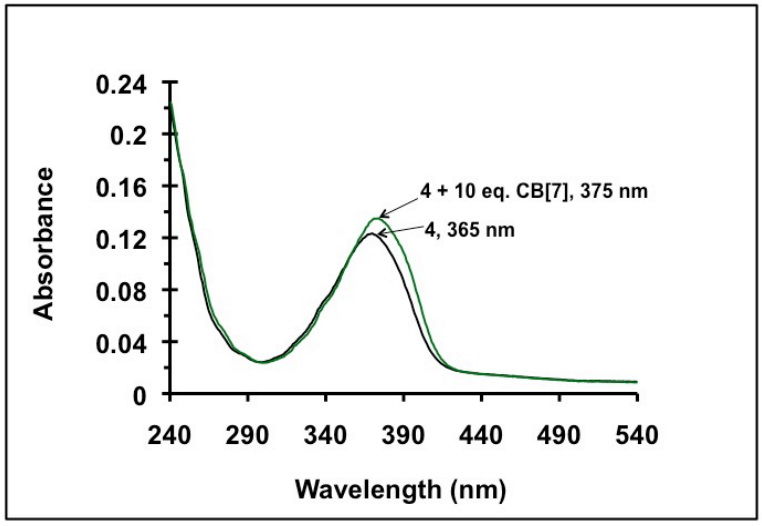

Figure S5. UV-vis absorption of control NMI **4** (1.0 x 10^{-5} M) with 10eq. CB[7] in ultrapure water.

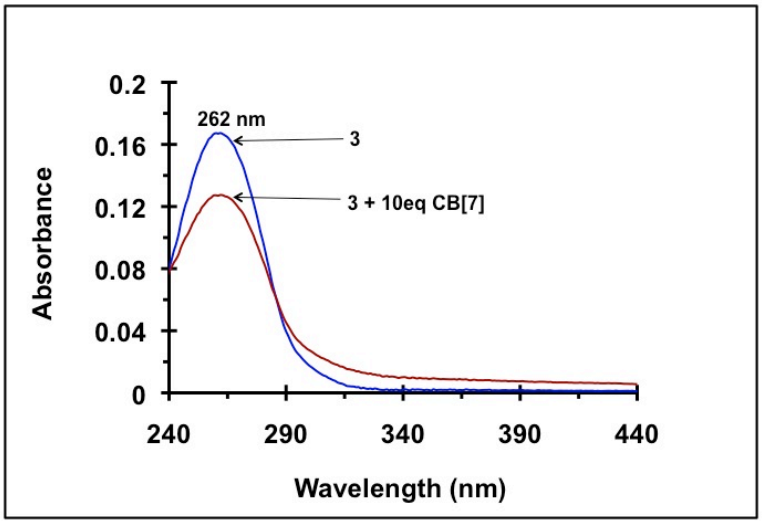

Figure S6. UV-vis absorption of control bpy **3** (1.0 x 10^{-5} M) with 10eq. CB[7] in ultrapure water.

Figure S2 shows that with no appended bipyridine moiety, the addition of CB[7] to NMI 4 shows only a moderate effect on the absorbance of the napthalimide chromophore at 365 nm, resulting in a slight increase and 10 nm red shift likely due to de-aggregation. Figure S3 shows the absorbance changes in bpy 3 on addition of CB[7], resulting in a significant decrease in absorbance at 262 nm suggesting that CB[7] is encapsulating the bpy moiety.

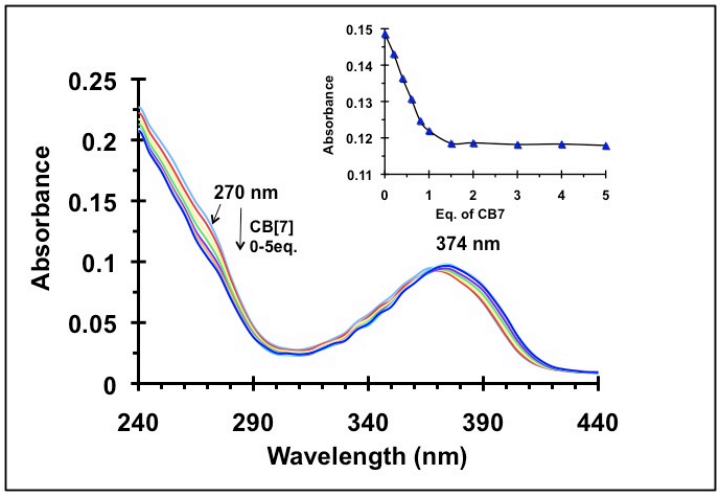

Figure S7. UV-vis absorption of NMI **1** (1.0 x 10^{-5} M) upon addition of 0- 5eq. CB[7] in ultrapure water. Inset: change in absorbance at 270 nm with CB[7] concentration.

Figure S4 shows the absorbance changes of NMI 1 on addition of CB[7]. The bipyridine absorbance at 270nm shows a decrease while the napthalimide absorbance shows only a red shift with no significant intensity change. These results, when taken together with the UV-vis data from the controls (Figures S2 & S3) support the notion that only the bpy unit of NMI **1** is included within CB[7].

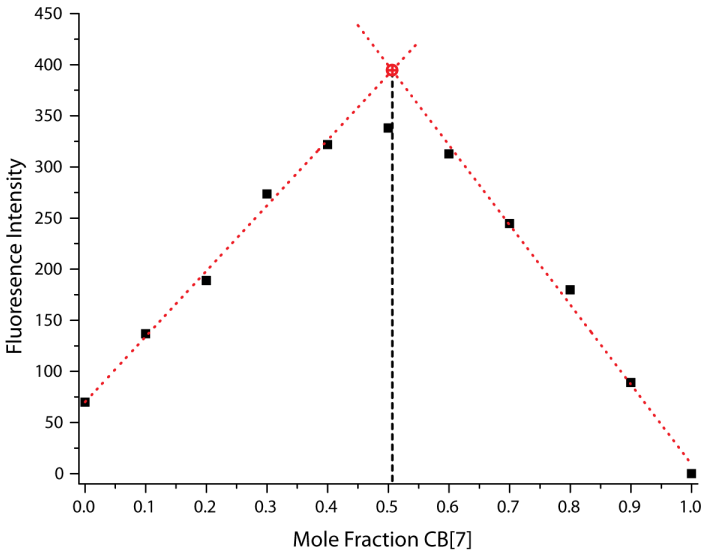

Figure S8. Job's plot of changes in fluorescence intensity by complexation between NMI **1** and CB[7] in ultrapure water. Total concentration of **1** and CB7 was kept constant at 2 μM. Intersection between lines is 0.5064, in good agreement with a 1:1 stoichiometry.

1.5.2 Fluorescence Quantum Yield Determination

Absorbance measurements were taken using a Hewlett Packard 8452A diode array spectrophotometer, and fluorescence spectra were obtained using a PTi Quantamaster 4 spectrophotometer fit with a Hammamatsu R928 PMT detector with quartz cuvettes. Quantum yields were determined from absorbance-corrected samples of NMIs **1** & **4**, as well as NMI **1** with CB[7] following standard methods.[4,5] Briefly, a well investigated standard (perylene) with excellent overlap of ground state absorption and emission with our samples was chosen. Samples were roughly absorbance matched to the standard at the excitation wavelength of 368 nm, followed by the collection of emission spectra, which were integrated using OriginPro 9.1 to obtain the integrated fluorescence intensity, *F*.

Quantum yields were determined by the following equation: [5]

$$\Phi_x = \Phi_{std}\left(\frac{F^x}{F^{std}}\right)\left(\frac{f_{std}}{f_x}\right)\left(\frac{\eta_x^2}{\eta_{std}^2}\right)$$

Where Φ_x and Φ_{std} are the quantum yields of the unknown and the standard, respectively, F is the integrated fluorescence intensity, f is the absorption factor ($f = 1\text{-}10^{-A}$, where A is the absorbance at 368 nm) and η is the refractive index.

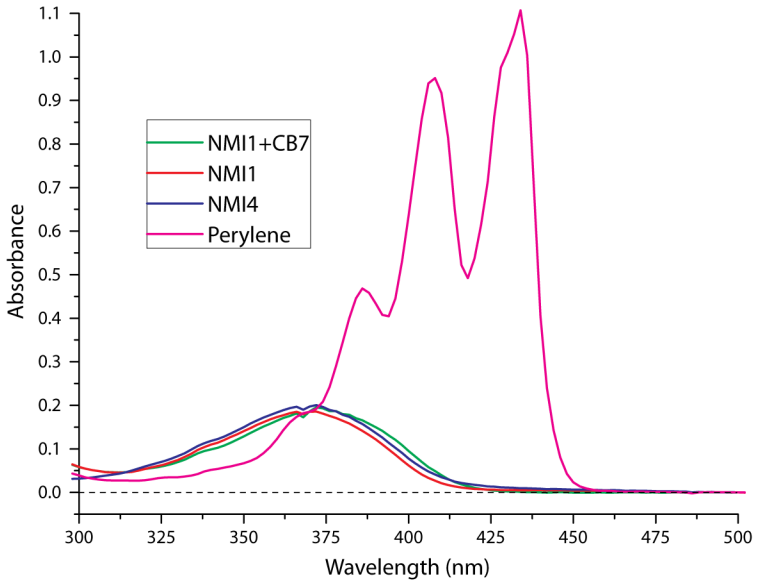

Figure S9. Absorbance overlays of perylene, **1**, **4**, and **1**+CB[7].

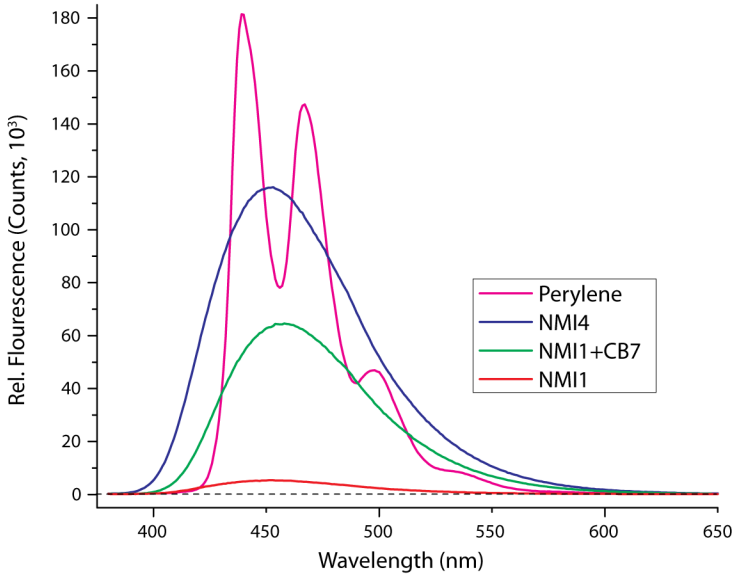

Figure S10. Fluorescence emission of **1**, **4**, **1**+CB[7] and perylene following excitation at 368 nm with 0.25 mm excitation monochrometer slit widths and 1.00 mm emission slit widths.

Table S1. Fluorescence quantum yields (Φ). Perylene 20 μM in absolute ethanol (η=1.36). NMI-1 & NMI-4 20 μM in H_2O (η=1.33). CB[7] 200 μM (10 equivalents).

	Perylene [4]	**NMI-4**	**NMI-1**	**NMI-1:CB[7]**
Integrated Fluorescence Intensity	7.98×10^6	9.55×10^6	4.49×10^5	5.28×10^6
[A] **Quantum Yield (Φ)** ± 5%	0.92	0.98	0.04	0.64

[A] Quantum yield values and standard error were calculated from the average values obtained from three trials.

1.5.3 Photophysical Data & Mechanism Discussion

Cyclic Voltammetry Methods: Voltammograms were obtained using a CH Instruments CHI730A Electrochemical Analyzer. The working electrode was a glassy-carbon electrode, the counter electrode was a Pt wire, and the reference electrode was an aqueous Ag/AgCl electrode. Data were collected in water solutions containing 0.1 M tetrabutylammonium chloride (TBACl) or acetonitrile solutions containing 0.1 M tetrabutylammonium hexafluorophosphate ($TBAPF_6$). All samples were deaerated with argon for 10 minutes prior to collection. An important consideration when performing electrochemical measurements is the electrochemical window of the solvent. This is the potential range over which the solvent is not reduced or oxidized. It was necessary to collect the oxidative electrochemistry of **1** in acetonitrile solution due to the limited oxidative potential window of water. In order to conduct these measurements in acetonitrile solution, **1** was isolated as the PF_6 salt via an anion exchange with $NaPF_6$.

Table S2. Redox Potentials of **1** and **1 with CB7** in H_2O and acetonitrile vs Ag/AgCl.

Complex	E^0 (2+/+) in CH_3CN (V) [A]	E^0 (+/0) in H_20 (V) [A]	ΔE_{CS} (V)[B]	E_{ES} (eV)[C]
NMI 1	1.92	-0.88	2.80	2.72
NMI 1 with CB7	1.92	-0.94	2.86	2.72

[A] The first, one-electron reduction and oxidation of the chromophore are both irreversible. The reported potentials are estimates of the half-wave potentials using the potential value when peak cathodic current is observed for the reduction potential (E^0 (+/0)) and peak anodic current is observed for the oxidation potential (E^0(2+/+)).

[B] $\Delta E_{CS} = E^0(2+/+) - E^0(+/0)$

[C] The excited state energy (E_{ES}) is obtained directly from the maximum of the luminescence spectrum of NMI 1 in H_2O. The value of 456 nm was first converted to wavenumbers and subsequently converted to electron volts (eV).

Time Correlated Single Photon Counting Measurements (TCSPC) Methods: Luminescence lifetimes were obtained using the time correlated single photon counting technique. Each sample was excited using an IBH NanoLED pulsed diode laser source (370 nm excitation, 200 ps pulse width). The emitted light was collected at right angle to the excitation pulse and collected by an IBH Model TBX-04 cooled photomultiplier (PMT) detector.

The output of the PMT served as the input for the stop channel of the time to amplitude converter (TAC, Tennelec TC-863). Start pulses for the TAC were obtained from the synchronous TTL output of the NanoLED laser source. The output from the TAC was directed to a multichannel analyzer (Ortec, Easy MCA) where the signal was accumulated. Laser light scattered from a cuvette containing water was used to accumulate the instrument response profile. Data sets were deconvoluted using the deconvolution routine in Origin 9.1. The luminescence decays from solutions of NMI 4 and NMI 1 with CB7 were fit using single exponential decay expressions. No specific lifetime values are provided for 1 in the absence of CB7 because the lifetime of the complex is shorter than the instrument response time of our experimental set-up (200 ps).

Table S3. Photophysical data for chromophores NMI 1, NMI 1 with CB7, and NMI 4. All data were collected in H_2O.

Compound	NMI 4	NMI 1	NMI 1 with CB7
Luminescence Quantum Yield (Φ_{lum}) ± 5%	0.98	0.04	0.64
Luminescence Lifetime (τ in ns)	7.7 ± 0.1	< 0.2 [A]	4.9 ± 0.1 [A]

[A] These values represent the lifetime of the system in equilibrium. A thorough discussion of this concept is found in the literature.[6]

Mechanism Discussion:

Given that viologen moieties are well known as electron acceptors and that 1,8-napthalimides have been shown to undergo photoinduced electron transfer (PET) when covalently linked to both dicationic and monocationic bypyridine units, [7,8] we believe that PET is responsible for the quenching observed in our NMI based sensors. In a PET mechanism, chromophores that contain moieties which can be oxidized and reduced by an initial excited state can result in a charge separated (CS) state. The thermodynamic feasibility of creating a CS state can be estimated using the first oxidation and reduction potentials of the particular system. If the sum of the energy (ΔE_{CS}) necessary to oxidize the donor (E^0 (2+/+)) and reduce the acceptor (E^0 (+/0)) is close to or below the energy of the initially formed excited state (E_{ES}), the formation of an equilibrium between the initial excited state and the CS state may be observed. For systems that experience an excited state equilibrium as described above, the lifetime of the overall system is a weighted average of lifetimes of the individual states and their relative percent contribution to the equilibrium; thus, population of a CS state generally results in a decrease in the

luminescence quantum yield of the initial excited state because charge recombination to form the ground state from the CS state is rapid relative to the luminescence from the chromophore.[6,9,10] All of the pertinent thermodynamic values for our systems are presented in Table S2. The energy of the initial, NMI localized excited state has an energy of 2.72 eV in H_2O. Electrochemical measurements reveal that the energy of the potential charge separated state of NMI 1 is 2.80 V for the free compound and 2.86 V for NMI 1 in the presence of CB7. An approximate equilibrium constant for each system can be determined from the estimated Gibbs Free Energy for the formation of the charge separated state ($\Delta G = -RTln(K_{eq})$). [9] For a system in which the charge separated state is 80 mV higher in energy than the initially created excited state, an equilibrium containing ~5% charge separated state is expected. Importantly, the addition of the CB7 increases the first electron reduction potential of the complex (see Table S2), resulting in an energy difference of 140 mV between the initial excited state and the CS state. For this case, we expect a less than ~1% contribution of the charge separated state to the excited state equilibrium. It follows that the enhanced contribution of the charge separated state to the decay of the excited state of the non-encapsulated version of NMI 1 leads to more dramatic quenching of the initially created excited state. Addition of CB7 to the system shifts the equilibrium to favor the initially created excited state, resulting in an enhancement in the luminescence observed from the system. This conclusion is supported by luminescence lifetime and luminescence quantum yield measurements. The control NMI 4 has a luminescence lifetime of 7.7 ± 0.1 ns and luminescence quantum yield of 0.98. Inclusion of the mono-cationic bipyridine (i.e., NMI 1) results in a luminescence quantum yield that is 25 times lower than that of NMI 4 and a luminescence lifetime value (< 200 ps) that is well over an order of magnitude shorter than NMI 4. Encapsulation of the bipyridine moiety increases the luminescence quantum yield to 0.64 with a corresponding luminescence lifetime value of 4.9 ± 0.1 ns.

1.6. Binding Studies

Binding studies for 1:1 CB[7] guest binding and sensor displacement assays were fit in Origin 9.1 using the method described by Uzunova [11] & Nau et al [12,13] with a scripting method described by Ansyln et al. [14]

1.6.1. 1:1 Binding

Given a Host (H) and a Guest (G) forming an inclusion complex (HG) with an equilibrium constant K_G, where [H] and [G] are the concentrations of free host and guest, respectively, and the total concentrations are $[H]_0$ and $[G]_0$:

$$K_G = \frac{[HG]}{[H][G]} \quad (1)$$

$$[G] = [G]_0 - [HG] \quad (2)$$

$$[H] = [H]_0 - [HG] \quad (3)$$

combining equations 1, 2 and 3 gives:

$$K_G = \frac{[HG]}{([G]_0 - [HG])([H]_0 - [HG])} \quad (4)$$

which can be re-arranged:

$$[HG]^2 + [HG]\left(-[G]_0 - [H]_0 - \frac{1}{K_G}\right) + [G]_0[H]_0 = 0 \quad (5)$$

which fits the form : $x^2 + bx + c = 0$, and gives as a solution:

$$x = \frac{-b - \sqrt{(b)^2 - 4c}}{2}, b = -[G]_0 - [H]_0 - \frac{1}{K_G}, c = [G]_0[H]_0, \text{ to give:}$$

$$[HG] = \frac{\left([G]_0 + [H]_0 + \frac{1}{K_G}\right) - \sqrt{\left([G]_0 + [H]_0 + \frac{1}{K_G}\right)^2 - 4[G]_0[H]_0}}{2} \quad (6)$$

$$[G] = [G]_0 - [HG], \Rightarrow [G] = \frac{[G]_0 - [H]_0 - \frac{1}{K_G} + \sqrt{\left([G]_0 + [H]_0 + \frac{1}{K_G}\right)^2 - 4[G]_0[H]_0}}{2} \quad (7)$$

In the course of the fluorescence titration, the total fluorescence signal (*Fl*) can be written as a linear combination of the mole fraction of each fluorescent species (ie, the partially quenched guest (I_G) and the fluorescent host-guest complex (I_{GH})). This in turn can be related to the concentration of guest in solution:

$$Fl = x_G I_G + x_{GH} I_{GH} = \frac{[G]}{[G]_0} I_G + \frac{[HG]}{[G]_0} I_{GH} = I_{GH} + (I_G - I_{GH}) \frac{[G]}{[G]_0} \quad (8)$$

Combining (7) and (8) yields the final equation to fit the intensity change to determine K_G:

$$Fl = I_{GH} + (I_G - I_{GH})\frac{[G]_0 - [H]_0 - \frac{1}{K_G} + \sqrt{\left([G]_0 + [H]_0 + \frac{1}{K_G}\right)^2 - 4[G]_0[H]_0}}{2[G]_0} \quad (9)$$

To fit the data, the values for I_{GH} and I_G are determined as the maximum and minimum values from the plot (completely complexed HG and complete free G, respectively) assuming the host has no intrinsic fluorescence. The total fluorescence of the system is then plotted vs. concentration of total host, $[H]_0$, given a total guest concentration $[G]_0$. The best fit is obtained with a slight (10%) allowance for variability of the I_G, and I_{GH} parameters.

1.6.2. Competitive Binding:

Given a Host (H), an indicating Guest (G), and a competitive guest (C) forming two competing inclusion complexes (HG & HC) with equilibrium constants K_G & K_C, with total and free concentrations of $[H]_0$, $[G]_0$ & $[C]_0$ and [H], [G] and [C], respectively:

$$K_G = \frac{[HG]}{[H][G]}, K_C = \frac{[HC]}{[H][C]} \quad (10)$$

$$[G] = [G]_0 - [HG] \quad (11)$$

$$[C] = [C]_0 - [HC] \quad (12)$$

$$[H] = [H]_0 - [HG] - [HC] \quad (13)$$

combining equation 10 with equation 11 or 12 yields:

$$[HG] = \frac{K_G[G]_0[H]}{1+K_G[H]}, [HC] = \frac{K_C[C]_0[H]}{1+K_C[H]} \quad (14)$$

which in combination with equation 13 yields:

$$[H] = [H]_0 - \frac{K_G[G]_0[H]}{1+K_G[H]} - \frac{K_C[C]_0[H]}{1+K_C[H]} \quad (15)$$

which can be re-arranged to yield equation 16.

$$K_C K_G[H]^3 + \left(K_C + K_G + K_C K_G([G]_0 + [C]_0 - [H]_0)\right)[H]^2 + (K_C([C]_0 - [H]_0) + K_G([G]_0 - [H]_0) + 1)[H] - [H]_0 = 0 \quad (16)$$

Equation 16 fits the form: $ax^3 + bx^2 + cx + d = 0$, with constants:

$$a = K_C K_G,$$

$$b = K_C + K_G + K_C K_G([G]_0 + [C]_0 - [H]_0),$$

$$c = K_C([C]_0 - [H]_0) + K_G([G]_0 - [H]_0) + 1,$$

$$d = -[H]_0$$

This cubic equation cannot be solved analytically, necessitating a computational solution. The Newton-Rhapson method solves a trinomial by using an iterative method, wherein the ratio of the polynomial to its first derivative should go to zero as the correct value of x is approached.

$$x_{n+1} = x_n - \frac{f(x_n)}{f'(x_n)} (17)$$

With a partially quenched guest with intensity I_G, and the fluorescent host-guest complex with intensity I_{GH}, the overall fluorescence intensity of the system can be written as a linear combination of the mole fraction of each fluorescing component with their intensity, which can in turn be related to the concentration of free host in solution:

$$Fl = x_G I_G + x_{GH} I_{GH} = \frac{[G]}{[G]_0} I_G + \frac{[HG]}{[G]_0} I_{GH} = I_G + (I_{GH} - I_G) \frac{K_G[H]}{1+K_G[H]} (18)$$

Given the intensity of the mixture, the polynomial (16) can be solved using the Newton method, and iteratively advanced by fit of the resulting value for [H] to the data using (18). The following code (written in labscript) will work with OriginPro 9.1 to script the fitting process:

```
a=kg*kc
b=kg+kc+kg*kc*GO-kg*kc*HO+kg*kc*CO
c=kg*GO-kg*HO-kc*HO+kc*CO+1
d=-HO

for (H=HO, step=1; abs(step)>1E-15; H=H-step){
 step=(a*H*H*H+b*H*H+c*H+d)/(3*a*H*H+2*b*H+c);};
f=Ig+((Igh-Ig)*(kg*H)/(1+kg*H))
```

The intensities of the free indicating guest (I_G) and complexed indicating guest (I_{GH}) along with the equilibrium constant for initial complexation (K_G) were determined by first fitting the 1:1 binding at the concentration of the indicating guest used in the competitive binding assay. Best fits were obtained when a 10% variation was allowed in the intensity parameters.

1.6.3. Validation of Binding Compared to Acridine Orange (AO)

To assess the effectiveness of NMI **1** as a sensor, the binding of CB[7] to a known guest (N-adamantylmethylbutane-1,4-diamine, AdButamine) was investigated in solution. In addition, the same experiment was conducted with AO as the sensor for validation purposes. First the binding of CB[7] to NMI **1** and AO was probed (Figure S8). Subsequently, the displacement of CB[7] from the sensors with AdButamine was investigated (AdButamine was synthesized according to the literature)[7] as shown in Figure S9.

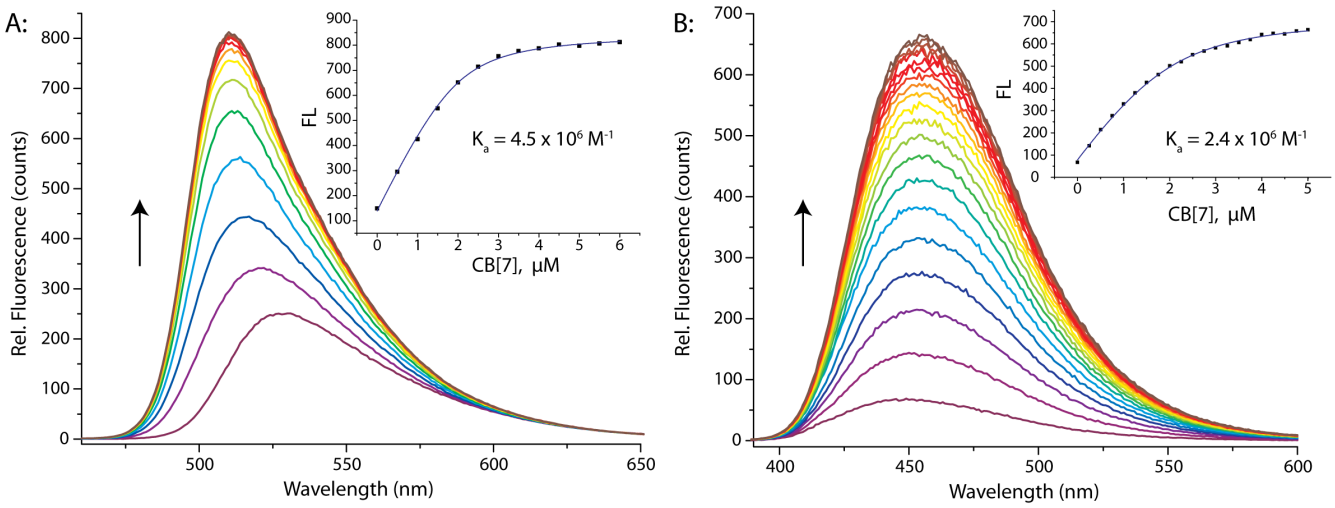

Figure S11: A) Binding of 2 µM AO with CB[7] in 10 mM ammonium phosphate buffer (7.2 pH), λ_{ex}=450 nm. Inset shows the fluorescence intensity as a function of CB[7] concentration plotted at λ=510 nm, fit to equation 9, yielding a K_a of 4.5 x 10^6 M^{-1}. B) Binding of 2 µM NMI **1** with CB[7] in 10 mM ammonium phosphate buffer (7.2 pH), λ_{ex}=365 nm. Inset shows the fluorescence intensity as a function of CB[7] concentration plotted at λ=455 nm, fit to equation 9, yielding a K_a of 2.4 x 10^6 M^{-1}.

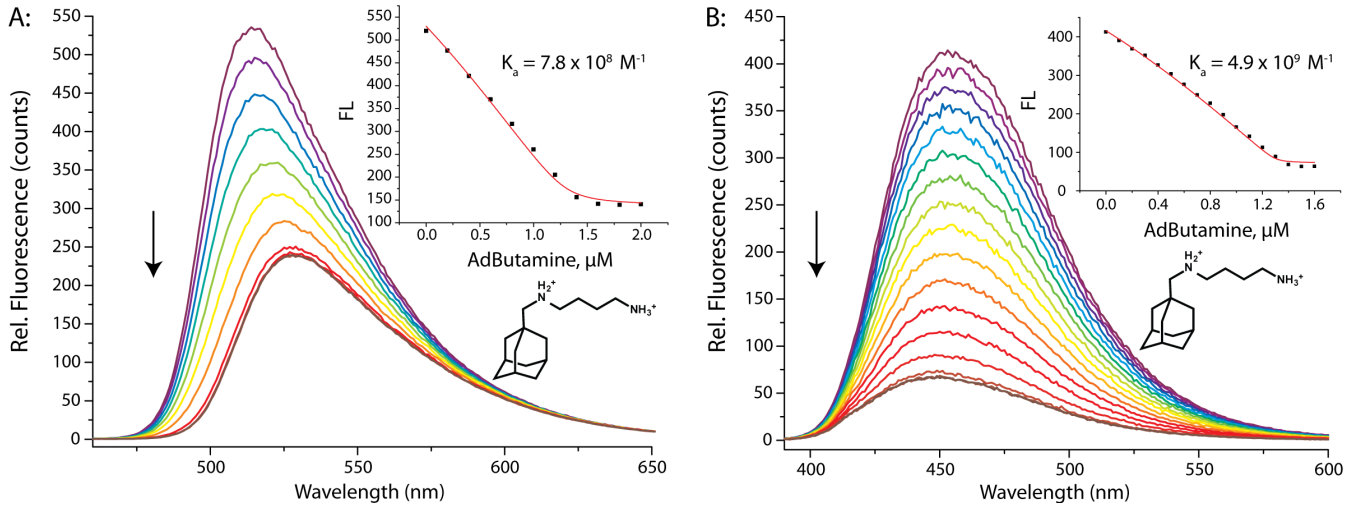

Figure S12: A) Displacement of 2 µM AO from 1.3 µM CB[7] with AdButamine in 10 mM ammonium phosphate buffer (7.2 pH), λ_{ex}=450 nm. Inset shows the fluorescence intensity as a function of AdButamine concentration plotted at λ=510 nm, fit to equation 18, yielding a K_a of 7.8 x 10^8 M^{-1} for AdButamine to CB[7]. B) Displacement of 2 µM NMI **1** from 1.3 µM CB[7] with AdButamine in 10 mM ammonium phosphate buffer (7.2 pH), λ_{ex}=365 nm. Inset shows the fluorescence intensity as a function of AdButamine concentration plotted at λ=455 nm, fit to equation 18, yielding a K_a of 4.9 x 10^9 M^{-1} for AdButamine to CB[7]. The two binding constants obtained with the different sensors are in good agreement with each other, as well as with the literature binding constant of (3±2) x 10^9 M^{-1}. [13]

1.7. Multi-Well Plate Studies

1.7.1 General Methods

All multi-well plate studies were performed on an EnSpire 2300 MultiMode plate reader using commercially available Streptavidin Coated High Capacity black 96-well plates from Pierce (#15503). Due to both the quantitative formation of the click adduct (**2**) and the specific nature of the plating via biotin-streptavidin binding, the crude click reaction sample was able to be directly used for assays without need for additional purification (i.e., the solid phase assay allows for the removal of any unbound reactants/catalysts via aqueous washes).

Figure S10 shows the general scheme for the multi-well assays on a per-well basis. Starting from the blank, streptavidin coated plate (Figure S10, 1) the crude NMI **2** was added at 100 µM (in 10% Aq. DMSO) and allowed to shake, covered, for 2 hours at room temperature (Figure S10, 2). To remove any un-bound NMI (as well as reactants/catalysts), the plate was washed (Figure S10, ii) 3x with 150 µL of a 100 mM Tris/25 mM NaCl buffer (7.2 pH) and then reconstituted with 180 µL of ultrapure water to yield the initially plated NMI **2** (Figure S10, 3). The initial equilibrated NMI **2** fluorescence reading was taken after 15 minutes at 25 °C. To form the encapsulated NMI **2**:CB[7] complex, 20 µL of a 1 mM CB[7] stock was added to each well (Figure S10, iii) (and mixed via pipette) to a final concentration of 100 µM. Following a 15 minutes equilibration at 25 °C° (during which the fluorescent readings plateaued), the equilibrated NMI **2**:CB[7] surface (Figure S10, 4) had a reading taken (F_0) as an initial "unquenched" data point for that specific well. Finally, 20 µL of each competitive guest (Figure S10, iv) was added and mixed via pipette to a final concentration of 100 µM. The final fluorescence reading for each well (F_G) was taken after a 15 minute equilibration at 25 °C. Raw data from the plate reader was collected, with a linear color scale allowing for rough approximation of initial binding strength relative to a row of known standards.

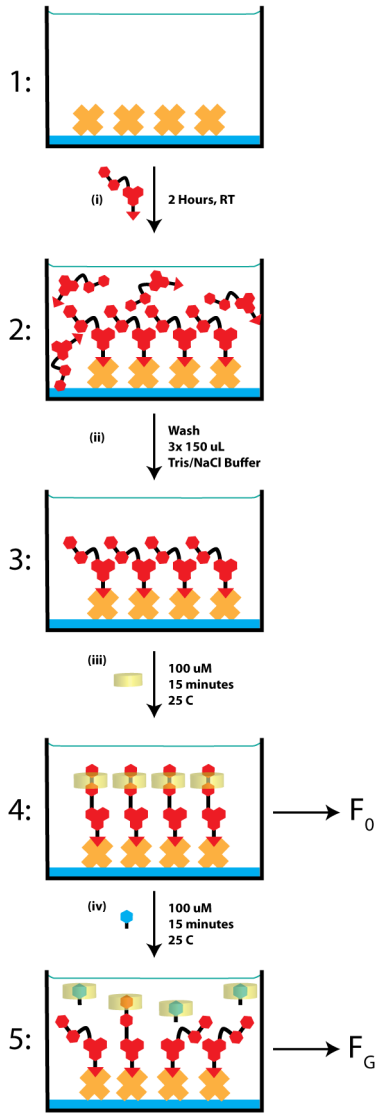

Figure S13: Scheme showing multi-well plate study.

To correct for differences between wells on a plate (in addition to between plates), data was converted from raw fluorescence to proportional quenching relative to the initial NMI **2**:CB[7] value (F_0) for that particular well. The ratio of F_G/F_0 (percent of initial fluorescence) was converted to a percent quenching by subtracting from 1. The positive control (NMI **2**:CB[7] in the absence of any competitive guests) shows a slight increase (~5%) over time (between the initial F_0 reading and the final F_G reading approximately 30 minutes later), resulting in a 'negative' percent quenching. The negative control (**2** alone) shows a strong decrease ranging from 89-92% quenching between replicates. For the final data plot, samples were assayed in triplicate over several days, and the percent quenching averaged across runs. Data for each run, as well as the average and standard deviation can be seen in Table S2.

Standards used all have known binding constants from the literature:

(B) 1,4-dimethyl-1,4-diazabicyclo[2.2.2]octane (Me_2DABCO, $K_a = 5 \times 10^5\ M^{-1}$),

(C) tetraethylammonium bromide (TEAB, $K_a = 1 \times 10^6\ M^{-1}$),

(D) N,N-dimethylmorpholine (Me_2Morph, $K_a = 5 \times 10^6\ M^{-1}$),

(E) N,N-dimethylpiperidine (Me_2Pip, $K_a = 3.7 \times 10^7\ M^{-1}$), and

(F) adamantylamine (AdAm, $K_a = 1.7 \times 10^{12}\ M^{-1}$) as cited in the main text.

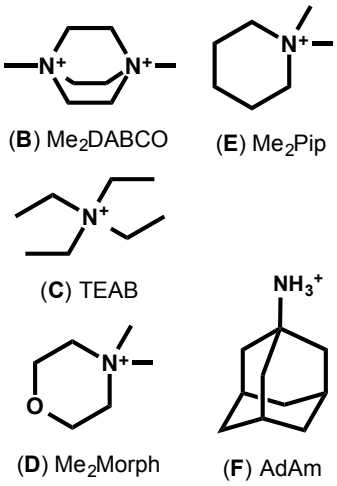

Table S2. All samples from multiwall plate assay, including results from all trials, averages and standard deviations. Percent quenching relative to the NMI **2**:CB[7] maximal fluorescence for that well. Novel binders are bolded.

Type	Row	ID	Trial 1	Trial 2	Trial 3	Average	StdDev
(1) Standard	A	NMI **2**+CB7	-5%	-4%	-5%	-5%	0%
(1) Standard	B	Me_2Dabco	29%	33%	27%	30%	2%
(1) Standard	C	TEAB	50%	53%	50%	51%	1%
(1) Standard	D	Me_2Morph	66%	65%	66%	66%	0%
(1) Standard	E	Me_2Pip	76%	77%	76%	76%	0%
(1) Standard	F	AdAm	80%	80%	81%	81%	0%
(1) Standard	G	NMI **2**	92%	93%	88%	91%	2%
(2) AntiCancer	B	Ifosfamide	23%	22%	22%	22%	0%
(2) AntiCancer	**C**	**Doxorubicin**	**64%**	**56%**	**69%**	**63%**	**5%**
(2) AntiCancer	D	Methotrexate	12%	20%	13%	15%	4%
(2) AntiCancer	E	5'Fluorouracil	12%	20%	16%	16%	3%
(2) AntiCancer	F	Oxaliplatin	84%	83%	83%	83%	0%
(2) AntiCancer	G	Fluvestrant	24%	20%	27%	24%	3%
(3) CAII Inhibitor	B	6-Ethoxy-2-benzothiazolesulfonamide	20%	20%	22%	21%	1%
(3) CAII Inhibitor	C	4-aminomethylbenzenesulfonamide	0%	-1%	-2%	-1%	1%
(3) CAII Inhibitor	D	Dorzolamide	14%	9%	13%	12%	2%
(3) CAII Inhibitor	E	Acetezolamide	3%	13%	14%	10%	5%
(3) CAII Inhibitor	**F**	**AdBenzSulfonamide**	**74%**	**73%**	**76%**	**74%**	**1%**
(3) CAII Inhibitor	G	Dansylamide	24%	17%	23%	21%	3%
(4) Antimalarial	B	Chloroquine	32%	27%	32%	30%	2%
(4) Antimalarial	C	Artmesinin	17%	12%	34%	21%	9%
(4) Antimalarial	D	Proguanil-HCl	17%	14%	16%	16%	1%
(4) Antimalarial	E	Cryptolepine	13%	3%	7%	8%	4%
(4) Antimalarial	F	Phenosafranin	40%	32%	47%	40%	6%
(4) Antimalarial	**G**	**N-(4-aminophenyl)piperidine**	**60%**	**45%**	**56%**	**54%**	**6%**

1.7.2. Validation of Novel Binders

Three novel binders to CB[7] were identified from the multi-well assay. Two were suspected to be of moderate binding affinity (doxorubicin & N-(aminophenyl)-piperidine (NAmPhenPip) and one of strong binding affinity (4-(adamantan-1-yl-carboxamido)-benzenesulfonamide (AdBenzSulfonamide). Each novel binder was validated by a solution phase displacement assay and binding constants were determined as described in section 1.6. Doxorubicin displacement titrations in solution (Figure S11), yield a K_a = 2.5 x 10^6 M^{-1}. N-(4-aminophenyl)-piperidine (Figure S12) displayed a good titration curve, yielding a binding constant of 1 x 10^7 M^{-1}. The remaining strong binder, AdBenzSulfonamide shows a binding constant of 1.3 x 10^9 M^{-1} (Figure S13).

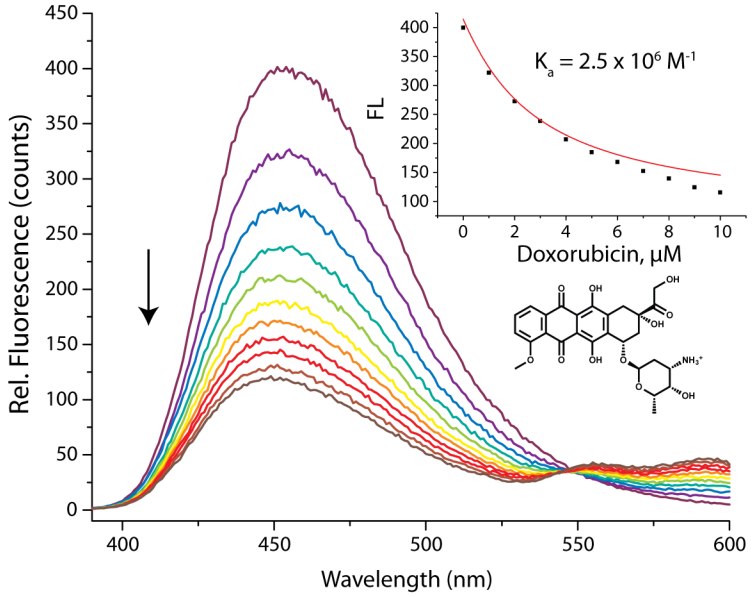

Figure S14: Displacement of 2 µM of theNMI **1** from 1.3 µM CB[7] with Doxorubicin in 10 mM ammonium phosphate buffer (7.2 pH), λ_{ex}=365 nm. Inset shows the fluorescence intensity as a function of Doxorubicin concentration plotted at λ=455 nm, fit to equation 18, yielding a K_a of 2.5 x 10^6 M^{-1} for Doxorubicin to CB[7].

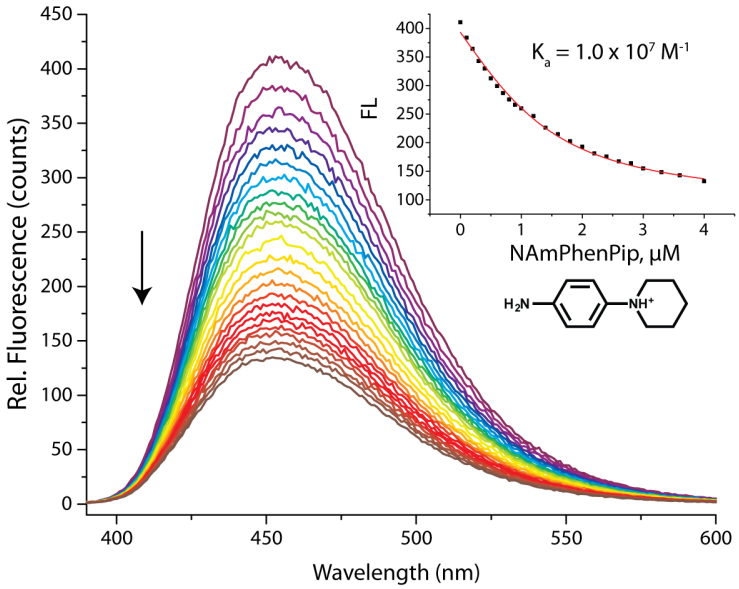

Figure S15: Displacement of 2 µM of the NMI **1** from 1.3 µM CB[7] with N-(aminophenyl)-piperidine (NAmPhenPip)in 10 mM ammonium phosphate buffer (7.2 pH), λ_{ex}=365 nm. Inset shows the fluorescence intensity as a function of NAmPhenPip concentration plotted at λ=455 nm, fit to equation 18, yielding a K_a of 1.0 x 10^7 M^{-1} for NAmPhenPip to CB[7].

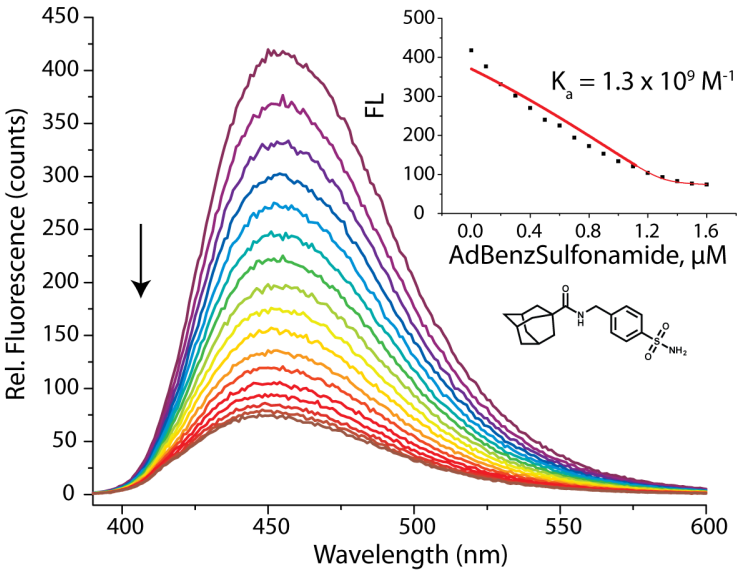

Figure S16: Displacement of 2 µM of the NMI **1** from 1.3 µM CB[7] with AdBenzSulfonamide in 10 mM ammonium phosphate buffer (7.2 pH), λ_{ex}=365 nm. Inset shows the fluorescence intensity as a function of AdBenzSulfonamide concentration plotted at λ=455 nm, fit to equation 18, yielding a K_a of 1.3 x 10^9 M^{-1} for AdBenzSulfonamide to CB[7].

1.8. References

1. Yi, S.; Kaifer, A. E. *J. Org. Chem*. **2011**, 76, 10275.
2. Ilies, M. A.; Masereel, B.; Rolin, S.; Scozzafava, A.; Campeanu, G.; Cimpeanu, G.; Cimpeanu, V.; Supuran, C. T. *Bioorg. Med. Chem*. **2004**, *12*, 2717.
3. Gamal-Eldin, M. A.; Macartney, D. H. Org. Biomol. Chem. **2013**, 11, 1234.
4. Brouwer Albert, M. In Pure Appl. Chem. 2011; Vol. 83, p 2213.
5. C. Würth, M. Grabolle, J. Pauli, M. Spieles and U. Resch-Genger, *Nat. Protocols*, 2013, **8**, 1535-1550.
6. T.A. Grusenmeyer, J. Chen, Y. Jin, J. Nguyen, J.J. Rack, R.H. Schmehl, *J. Am. Chem. Soc,* 2012, **134**, 7947-7506.
7. T. P. Le, J. E. Rogers and L. A. Kelly, *The Journal of Physical Chemistry A*, 2000, **104**, 6778-6785.
8. L. Zhu, M. Lu and H. Tian, *Tetrahedron*, 2012, **68**, 79-84.
9. W.E. Ford, M.A. Rodgers, *J. Phys. Chem.*, 1992, **96**, 2917-2920.
10. T.A. Perkins, W. Humer, T.L. Netzel, K.S. Schanze, *J. Phys. Chem.*, 1990, **94**, 2229-2232.
11. Uzunova, V. D. Thermodynamic and Fluorescence-based Investigations of Host-Dye Reporter Pairs for Sensing of Biological Analytes. Jacobs University, **2011**.
12. Hennig, A.; Bakirci, H.; Nau, W. M. *Nat Meth.* **2007**, 4 (8), 629-632.
13. Hennig, A.; Hoffmann, A.; Borcherding, H.; Thiele, T.; Schedler, U.; Resch-Genger, U. *Chem. Commun.* (Cambridge, U. K.) **2011**, 47 (27), 7842-7844.
14. Hargrove, A. E.; Zhong, Z.; Sessler, J. L.; Anslyn, E. V. *New J. Chem*. **2010**, 34 (2), 348-354.